The Journal of Experimental Biology 210, 2811-2818
Published by The Company of Biologists 2007
doi:10.1242/jeb.004267

Death roll of the alligator: mechanics of twist feeding in water

Frank E. Fish[1,*], Sandra A. Bostic[1], Anthony J. Nicastro[2] and John T. Beneski[1]
[1]*Department of Biology and* [2]*Department of Physics, West Chester University, West Chester, PA 19383, USA*
*Author for correspondence (e-mail: ffish@wcupa.edu)

Accepted 14 May 2007

Summary

Crocodilians, including the alligator (*Alligator mississippiensis*), perform a spinning maneuver to subdue and dismember prey. The spinning maneuver, which is referred to as the 'death roll', involves rapid rotation about the longitudinal axis of the body. High-speed videos were taken of juvenile alligators (mean length=0.29 m) performing death rolls in water after biting onto a pliable target. Spinning was initiated after the fore- and hindlimbs were appressed against the body and the head and tail were canted with respect to the longitudinal body axis. With respect to the body axis, the head and tail bending averaged 49.2° and 103.3°, respectively. The head, body and tail rotated smoothly and freely around their individual axes of symmetry at 1.6 Hz. To understand the dynamics of the death roll, we mathematically modeled the system. The maneuver results purely from conservation of angular momentum and is explained as a zero angular momentum turn. The model permits the calculation of relevant dynamical parameters. From the model, the shear force, which was generated at the snout by the juvenile alligators, was 0.015 N. Shear force was calculated to scale with body length to the 4.24 power and with mass to the 1.31 power. When scaled up to a 3 m alligator, shear force was calculated at 138 N. The death roll appears to help circumvent the feeding morphology of the alligator. Shear forces generated by the spinning maneuver are predicted to increase disproportionately with alligator size, allowing dismemberment of large prey.

Key words: death roll, alligator, *Alligator mississippiensis*, feeding, maneuverability.

Introduction

Crocodilians, including the American alligator *Alligator mississippiensis*, are large aquatic predators. These reptiles approach their prey with stealth and forcefully grab the prey with their conical teeth and large jaws (Davenport et al., 1990; Cleuren and De Vree, 1992; Cleuren and De Vree, 2000; Erickson et al., 2003). Although small prey are swallowed whole, large prey are subdued and dismembered with a spinning maneuver (McIlhenny, 1935; Neill, 1971; Guggisberg, 1972; Pooley and Gans, 1976; Ross, 1989). This maneuver is dramatically termed the 'death roll'. The death roll is an example of a behavioral strategy referred to more generally as rotational feeding.

Body-rolling inertial feeding or rotational feeding is used by elongate vertebrates that lack specialized cutting dentition (Gans, 1974; Helfman and Clark, 1986; Davenport et al., 1990; Maesey and Herrel, 2006). The inability to cut food into smaller portions requires such species to use mechanisms to remove manageable pieces from prey that are too large to consume whole. Large crocodiles and alligators will grab a limb or lump of flesh with their jaws and then rotate around the longitudinal axis of their body until the piece is torn free (Guggisberg, 1972; Cleuren and De Vree, 2000). While there have been numerous observations of the spinning behavior for prey reduction, there is only one description of the gross motions of the body components for the alligator (McIlhenny, 1935). McIlhenny reported that an alligator would immediately roll when it caught an animal that was too large to be instantly killed. The alligator would initiate the roll by throwing its tail up and sideways. The body and tail would turn simultaneously in the same direction. The feet were not used as they were folded against the body. Observations from a second crocodilian species, large (>3 m) Nile crocodiles, *Crocodylus niloticus*, reported spin rates of 0.55–1.11 rotations s^{-1} (Helfman and Clark, 1986).

The mechanics of the spinning maneuver in crocodilians have not been previously examined. The goal of this study was to understand how the alligator is able to initiate and sustain a spinning maneuver in an aquatic medium and to construct a model to describe the relevant dynamics. In this study, we were able to elicit juvenile alligators in the laboratory to spin in the manner of the death roll. By using high-speed video recordings of the rolling maneuver, we detailed the movements of body components and measured spinning performance. From this information, a mathematical model was produced that satisfactorily described the dynamics of the rolling maneuver, allowing the model to predict the torque and shear forces produced at the snout during this feeding behavior.

Materials and methods

Nine juvenile alligators *Alligator mississippiensis* Daudin were purchased from a commercial alligator farm (Everglades Outpost, Homestead, FL, USA). Each alligator was weighed,

Table 1. *Morphometric data for A. mississippiensis juvenile and adult forms*

Model parameter	Ellipsoidal head	Ellipsoidal body	Conical tail
Juvenile (*N*=9)			
a (m)	0.023	0.047	*l*=0.16
b (m)	0.015	0.015	*r*=0.0075
c (m)	0.015	0.015	
m (kg)	0.0144	0.0391	0.0098
i (kg m^2)	1.3×10^{-6}	3.5×10^{-6}	1.6×10^{-7}
I (kg m^2)	2.2×10^{-6}	1.9×10^{-5}	9.5×10^{-6}
Adult (*N*=1)			
a (m)	0.48	0.90	*l*=1.60
b (m)	0.25	0.33	*r*=0.23
c (m)	0.25	0.33	
m (kg)	17.35	65.93	32.39
i (kg m^2)	0.43	2.87	0.51
I (kg m^2)	1.02	12.12	3.37

For an explanation of the symbols, please see List of symbols and abbreviations.

measured, and sketched for identification. Morphometrics of the alligators are provided in Table 1. The total body length (mean ± s.d.; tip of rostrum to tip of tail) and body mass were 299±9 mm and 66±8 g, respectively. One animal, which died, was used to determine the relative proportions of mass for the head, body and tail. The animals were housed together in a large aquarium (1.23 m×0.46 m×0.53 m) that was filled with water to a height of 50 mm. Bricks placed in the aquarium acted as islands where the alligators could rest out of the water. Alligators were maintained at 21–22°C with a light cycle of 12 h:12 h L:D. Animals were supplied with a diet of live earthworms (*Lumbricus terrestris*) and strips of beef.

Experiments on spinning were conducted in a 38 l aquarium (0.51 m×0.26 m×0.32 m). Water depth was 100 mm, which was sufficient to keep the alligator from touching the bottom of the aquarium with any part of its body. Water temperature was 20–23°C. Alligators were placed singly in the test aquarium and allowed to acclimate for a minimum of 10 min. Immediately upon entry into the aquarium, the alligator would dive and swim. The alligator would eventually return to the water surface where it would float quiescently. The alligator would be presented with a small (approximately 50 mm) strip of meat held with tongs at the water surface. Once the animal grasped the meat, one to several small, sharp tugs were given to induce it to spin.

To determine if motions or orientation of the tail were associated with spinning, the tails of the alligators were restrained. Two test groups of four animals each were chosen. Strips of duct tape were used to bind a wooden stick (180 mm×6 mm×1 mm) to the dorsum of the alligators in one group (Fig. 1) and the venter of alligators in the other group. The neck and legs were free to move in all animals. The alligators were able to float at the water surface. As with unrestrained alligators, these animals were presented with a strip of meat to bite in order to initiate spinning. Restrained alligators were tested for no longer than 10 min.

Fig. 1. Juvenile alligator showing tail restraint. The wooden stick on the dorsum of the alligator is 180 mm in length.

The spinning maneuver was recorded with a high-speed video camera (Redlake Imaging MotionMeter, Morgan Hill, CA, USA) at 250 frames s^{-1} with a 6 mm lens (Cosmicar Television Lens, Japan). The camera was mounted on a tripod 1.6 m above the aquarium. Video recordings from the camera were played back at 60 frames s^{-1} and stored on videotape using a Panasonic AG-7300 video recorder. Two 250 W halogen lamps supplied lighting at water level.

Sequential frames of videotape were viewed using a Panasonic CT 2600 M monitor and Panasonic AG 7300 video recorder. Video records were chosen for analysis only if the animal displayed at least one full rotation, the animal was not pushing off the walls or floor of the aquarium, and the entire animal was in the field of view. Each spinning sequence was analyzed frame-by-frame. Data were collected on the duration of a complete spin, number of spins, and angular displacements of the head and tail relative to the longitudinal axis of the body. Angular displacements were measured using a protractor on the video frame at the initiation of the spin when the animal's dorsum was directed toward the camera and the animal's head, body and tail were parallel to the plane of the water surface. These angular data were combined with the morphometrics data to construct a mathematical model that allowed calculation of torques and shear forces, resulting from death roll behaviors.

Results

Live animals

A total of 52 sequences of spinning by unrestrained alligators was recorded. Spinning was induced by tugging on the meat, and spinning stopped when the alligator succeeded in tearing off a section of meat. Each sequence contained either one (73%), two (17%), or three (10%) complete spins. In every instance, the meat was proffered directly at the snout tip. Because the alligator did not move to approach the target meat, the animal did not initially possess any linear or angular momentum. This experimental condition of zero initial angular momentum will be important to understand the mechanics of the death roll.

Sequential images of spins are shown in Figs 2 and 3. The spin was observed after limbs and tail were moved (Fig. 2). The head, body and tail were bent into a C-shape. The fore- and hindlimbs were appressed against the sides and venter of the body. The head and tail could be flexed laterally, dorsally, or ventrally. Once the spin was initiated, the body remained

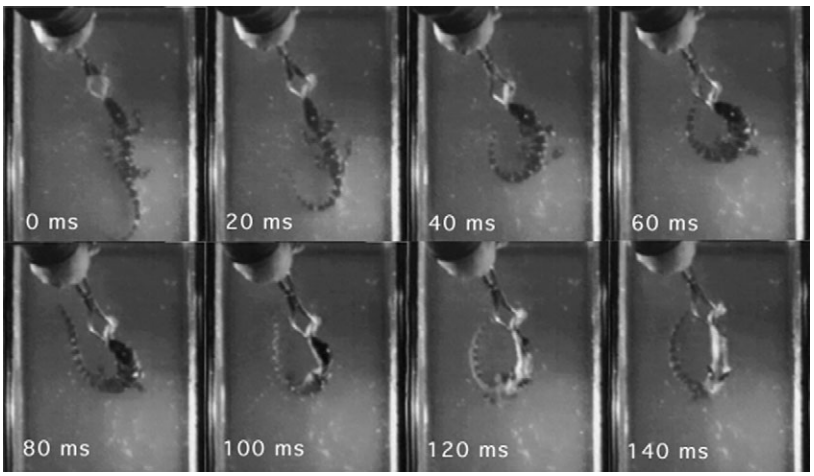

Fig. 2. Initiation (0 ms) of the spinning maneuver. The alligator first bends into a C-shape and then appresses its limbs against the body.

relatively straight from the pectoral region to the pelvic region (Fig. 3). The alligator maintained this shape throughout the maneuver. The head, body and tail rotated around their individual longitudinal axes. The tail was rotated at its base, maintaining its position throughout the spin. However, the relative orientation of the body parts change with respect to each other. In Fig. 2, the tail starts bent to the left side of the alligator, but is bent to the right side of the animal later in the spin. At the end of the spin, the head, body and tail straighten out. In all cases, the legs abduct from the body and return to a typical sprawled posture, thus ending with zero angular momentum. With this condition, there are no external torques or forces operating during the spinning maneuver. Drag from the interaction of the animal and the fluid is thus negligible. In a few cases, after the animal straightens at the end the maneuver, a slow residual spin remains. This small amount of angular motion was attributed to an inadvertent external torque applied in the feeding.

The angle (θ) between the longitudinal axes of the head and body at the start of each maneuver ranged between 20° and 75° with a mean of 49±10° (Fig. 4). The angle (ϕ) between the body and tail at the same time ranged between 79° and 139° with a mean of 103±13° (Fig. 4). There was no significant correlation between head and tail angles (d.f.=50; R=0.043). The mean rate of rotation was 1.5±0.5 rotations s^{-1} or 560±170° s^{-1}. The rotation rate ranged from 0.7 to 2.7 rotations s^{-1} (257–978° s^{-1}) No significant correlations were found for head or tail angle with rotation rate (head: d.f.=50; R=0.131; tail: d.f.=50; R=0.184).

When the tail was restrained, alligators could not be induced to spin. In all cases, the legs were never tucked against the body.

Model

Based upon the observations and kinematics of the spinning maneuver, a mathematical model was developed that was based on a spinning maneuver with a zero not angular momentum. Such zero angular momentum turns have been analyzed for some simple cases, such as a falling cat and aerial human maneuvers (Kane and Scher, 1970; Frohlich, 1979; Edwards, 1986; Galli, 1995). The dynamics of our model permit a calculation of the torque and shearing force produced at the snout.

The alligator was modeled as ellipsoidal head and body with a right circular cone as a tail (Fig. 5). The head and body had circular cross sections. The joints at the junctions of head and body and the body and tail can rotate freely without slipping. As indicated above, the initial state is one of zero angular momentum. The head and body sections each possess three principal moments of inertia. For the model head with semi-

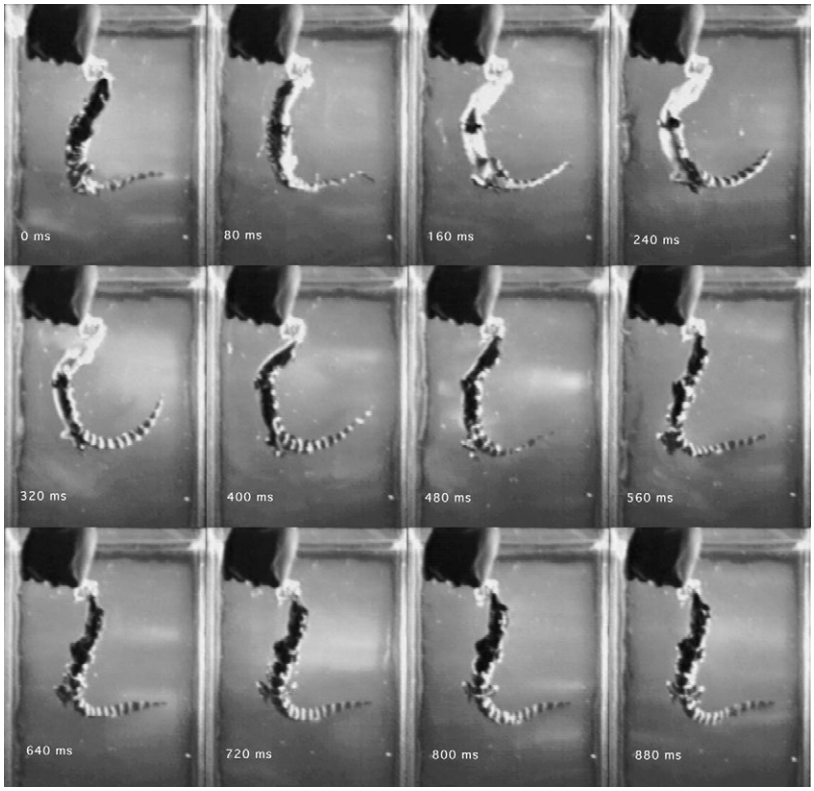

Fig. 3. Spinning maneuver of juvenile alligator after initiation (0 ms). The alligator has bitten onto a piece of meat. During the spinning maneuver, the rotational axes of the head, body and tail maintain a fixed relative orientation to the frame of reference of the aquarium. Note that the relative orientation of the body parts do change with respect to each other. For instance, the tail starts bent to the left side of the alligator at 20 ms, but is bent to the right side of the animal by 120 ms, although still on the left side of the image. The limbs are appressed against the body and the head and tail are canted at angles to the body axis. The head, body and tail all spin in the same rotational direction with the same angular speed.

major axis of a_H and semi-minor axes each of length b_H, we denote the smallest moment of inertia about the major axis as i_H. The moments about the two equal minor axes are each denoted by I_H and are larger than the moment about the major axis (Table 1). The length of the head l_H is $2a_H$ and the width and thickness are each $2b_H$. In this case,

$$i_H = \frac{m_H}{5}(b_H^2+b_H^2) = \frac{m_H}{5}(2b_H^2) \quad (1)$$

and

$$I_H = \frac{m_H}{5}(a_H^2+b_H^2)\,, \quad (2)$$

where m_H is the mass of the head alone (Gray, 1963). Similarly for the model ellipsoidal body (or trunk) with axes of length a_B and b_B, the principal moments of inertia i_B and I_B are given by:

$$i_B = \frac{m_B}{5}(b_B^2+b_B^2) = \frac{m_B}{5}(2b_B^2) \quad (3)$$

and

$$I_B = \frac{m_B}{5}(a_B^2+b_B^2)\,. \quad (4)$$

For the model right circular cone tail, the three principal moments are i_T and I_T given by:

$$i_T = \frac{3}{10}m_T r^2 \quad (5)$$

and

$$I_T = \frac{3}{20}m_T\left(r^2+\frac{l_T^2}{4}\right), \quad (6)$$

where m_T is the mass of the tail, r is its radius at the base, and l_T is its length.

The model head, body and tail all roll without slipping with angular speeds $\omega_H=\omega_B=\omega_T=\omega$ and simultaneously revolve around the RR′-axis, the roll axis, with angular speed ω_{rev} (Fig. 5).

The rotating head, body and tail each possess angular momentum. To determine the moments of inertia of the body parts and the resulting angular momenta about the RR′-axis, we adopt the coordinate system shown in Fig. 5. The unit vectors for each body part are described in Cartesian coordinates of $\hat{x}$ and $\hat{y}$. The $\hat{y}$ axes lie along the spin axes of each body part and the $\hat{x}$ axes are perpendicular to the $\hat{y}$ axes. The angular momentum of the head is:

$$\overrightarrow{L_H} = i_H\omega\hat{y}_H - i_H\omega_{rev}\cos\theta\hat{y}_H + I_H\omega_{rev}\sin\theta\hat{x}_H\,. \quad (7)$$

Similarly, for the body and tail, respectively,

$$\overrightarrow{L_B} = -i_B\omega\hat{y}_B - (i_B+m_Bd^2)\omega_{rev}\hat{y}_B\,, \quad (8)$$

$$\overrightarrow{L_T} = i_T\omega\hat{y}_T - i_T\omega_{rev}\cos\phi\hat{y}_T - I_T\omega_{rev}\sin\phi\hat{x}_T\,. \quad (9)$$

The parallel axis theorem was used to determine the moment of inertia of the body revolving around the RR′-axis, which is a distance d away from the longitudinal axis of the body.

In a zero angular momentum maneuver, the vector sum of these angular momenta vanishes, that is, $\overrightarrow{L_H}+\overrightarrow{L_B}+\overrightarrow{L_T}=0$. For this case,

$$0 = \omega_{rev}(I_H\hat{x}_H\sin\theta - I_T\hat{x}_T\sin\phi) + \omega(i_H\hat{y}_H+i_T\hat{y}_T) + \omega i_B\hat{y}_B - \omega_{rev}(i_H\hat{y}_H\cos\theta+i_T\hat{y}_T\cos\phi) - \omega_{rev}(i_B+m_Bd^2)\hat{y}_B\,. \quad (10)$$

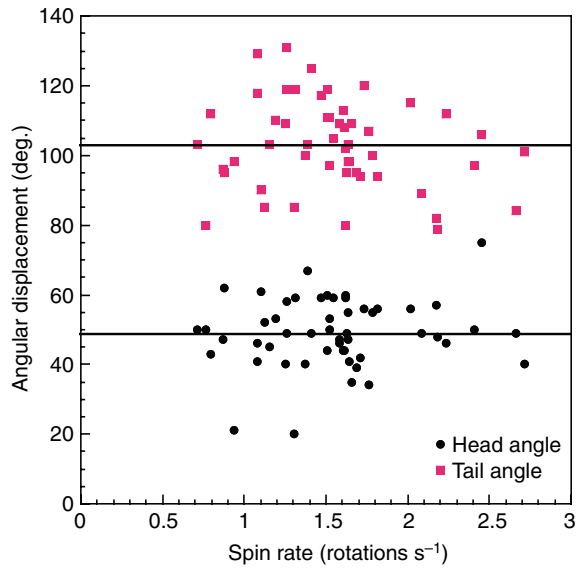

Fig. 4. Angular displacement of head and tail to symmetry axis of body in relation to spin rate. Solid lines indicate mean angles for the head and tail.

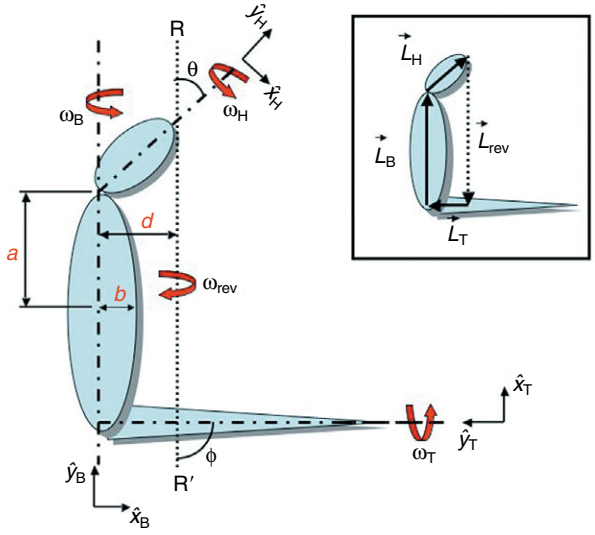

Fig. 5. Model of alligator during spinning maneuver. The head and tail are modeled as ellipsoids with circular cross sections. The tail is modeled as a elongate right circular cone. The semi major (a) and semi minor (b) axes of ellipsoids are exemplified on the body. Angular displacements of the head (θ) and tail (ϕ) are shown relative to the symmetry axis of the body. Angular velocities (ω_H, ω_B, ω_T) of body parts rotate together. The local Cartesian coordinate system is illustrated along the symmetry axis for each body part. The roll axis (RR′) is indicated by the broken line at a distance (d) from the symmetry axis of the body. The angular velocity (ω_{rev}) around the roll axis is opposite in direction to the angular velocities of the body parts. The inset illustrates the vector angular momenta for the entire system. The vector sum of the angular momenta is zero for the motions of the alligator during the spinning maneuver.

If the total angular momentum of a system is zero, it is zero about any axis. The angular momentum projected onto the RR′-axis is therefore:

$$0 = \omega_{rev}(I_H\sin^2\theta - I_T\sin^2\phi) + \omega(i_H\cos\theta + i_T\cos\phi) + \omega i_B - \omega_{rev}(i_H\cos^2\theta + i_T\cos^2\phi) - \omega_{rev}(i_B + m_B l_H^2\sin^2\theta)\,, \quad (11)$$

where we have used the fact that $d = l_H\sin\theta$ with l_H the length of the head. After rearranging terms to form the ratio ω/ω_{rev}, we find:

$$\omega/\omega_{rev} = \frac{i_H\cos^2\theta + i_T\cos^2\phi + (m_B l_H^2 - I_H)\sin^2\theta + I_T\sin^2\phi + i_B}{i_H\cos\theta + i_T\cos\phi + i_B}\,. \quad (12)$$

However, for $\theta = 45°$ and $\phi = 90°$, which are typical values for these angles (Fig. 4), this expression reduces to:

$$\omega/\omega_{rev} = \frac{i_H + 2i_B + m_B l_H^2 - I_H - 2I_T}{\sqrt{2}i_H + 2i_B}\,. \quad (13)$$

This expression is consistent with the observed characteristics of the death roll (see below).

It is important to note that the ω_{rev} motion (i.e. the motion of the animal revolving around the RR′-axis) is a reaction to the rolling motions initiated by the animal after it fastens onto its prey. Before the spin is initiated the angular momentum of the alligator is observed to be zero, must remain zero during the spin, and is observed to be zero when the spin terminates. The motion around the RR′-axis, which occurs at an angular frequency approximately an order of magnitude slower than the rolling motions, results purely from the conservation of angular momentum. This is roughly analogous to how a figure skater controls spin rate (Giancoli, 1985). By voluntarily bringing both arms close to his or her body from an extended position, a figure skater can increase angular speed to conserve angular momentum. Rather than this one-dimensional case, the death roll is a two-dimensional example.

Discussion

Significance of prey inertia to crocodilian spin feeding

Spinning is a maneuver to reduce large prey to small enough pieces that a crocodilian can swallow (McIlhenny, 1935; Neill, 1971; Guggisberg, 1972; Pooley and Gans, 1976; Ross, 1989). The conical teeth of crocodilians are useful for grasping prey with a large bite force (Erickson et al., 2003), but not for tearing and cutting flesh (Guggisberg, 1972). Spinning is a mechanism that can tear apart large prey by subjecting the tissue to torsional stresses. Animals and their tissues are weak in torsion (Gordon, 1978; Currey, 2002). The spinning maneuver is used predominately by crocodilians with broad, short snouts, which feed on large prey and on a more general diet (Cleuren and De Vree, 2000). This skull structure can resist the substantial forces associated with the maneuver (Cleuren and De Vree, 1992). Inertia of the prey is required for the maneuver to be effective. Spinning does not work with small prey animals, because as the crocodile spins, the prey will also rotate. Thus, when groups of crocodilians (e.g. *Crocodylus niloticus*) feed on a carcass at the same time (Pooley and Gans, 1976; Guggisberg, 1972; Ross, 1989), the inertia added by attached predators would facilitate the success of spin feeding by individual crocodilians by helping to secure the prey.

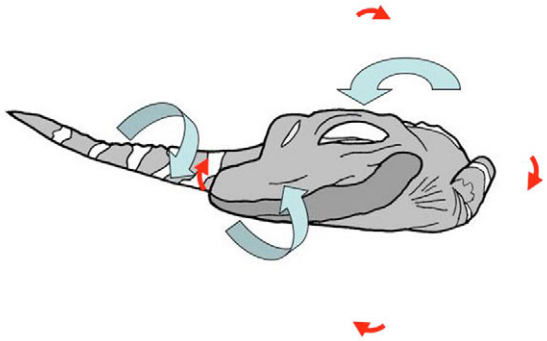

Fig. 6. Schematic of spinning motions. Blue arrows indicate directions of rotation of head, body and tail segments. Red arrows indicate compensatory rotation of the entire system. The relative size of the arrows illustrates a reduced rate of rotation of the compensatory spin compared to the rotation rates of the head, body and tail segments.

We discovered that juvenile alligators are capable of performing the death roll. Previous reports of spinning were associated with large crocodilians subduing or dismembering large prey items (McIlhenny, 1935; Pooley and Gans, 1976). Hatchling (50 g) and juvenile (100–550 g) salt-water crocodiles (*Crocodylus porosus*) feeding on carrion were observed to use side-to-side head shaking, rather than spinning, to detach small pieces (Davenport et al., 1990). Side-to-side head shaking was used to detach small pieces of the carrion. However, the carrion was a large fish, which may not have offered resistance to tearing (Davenport et al., 1990). The toughness of the food presented to the alligators in this study provided sufficient resistance to initiate the spinning behavior.

Conservation of angular momentum in crocodilian death rolls

The ferocity of the death roll of alligators and crocodiles is particularly enhanced by the rapid speed of the spinning motions. How can the animal generate these motions and still conserve angular momentum? From a configuration where the symmetry axes of the head, body and tail are all aligned, the animal quickly bends itself into a C-shape and commences spinning. Consequently, each body part possesses a vector angular momentum (Fig. 5). While the horizontal components of the angular momenta of the head and tail largely cancel, the vertical components add. This angular momentum vector, however, is canceled by a more subtle motion of the entire animal. As a reaction to the spinning motion, the animal also revolves around a roll axis roughly parallel to the animal's trunk (body). The roll axis runs through its snout, which is fastened onto meat, and a point approximately one-quarter of the distance from base of the tail to its tip. The revolution of the animal's head, body and tail about the roll axis also has an angular momentum, which is directly opposite to the vector sum of the angular momentums of each body segment. Thus, the initial angular momentum is zero, the total angular momentum during the roll is zero, and when the maneuver terminates by the alligator straightening, it remains zero.

The reason that the motion about the roll axis is less apparent than the spinning motions of the head, body and tail is because

it takes place with an angular speed that is an order of magnitude smaller than the spinning motion (Fig. 6). When an animal executes a roll of one spin, it only completes a tenth of a revolution around the roll axis. This relatively small angular velocity is not measurable in this experiment. The relatively small magnitude of this compensatory rotation can ultimately be attributed to the large size of the moment of inertia of the alligator bent into a C-shape with the massive trunk relatively far from the roll axis.

The alligator is able to centralize its mass and its axis of rotation by keeping its legs in close to its body. This also effectively helps reduce drag and enables it to create a faster, more powerful spin. Similarly, human divers create a central axis as they somersault from a diving board (Frohlich, 1980). By drawing their arms and legs in close to their body, they can isolate their axis of rotation. The same principle applies when a person is spinning on ice skates. When their arms are extended the spin is slowed down, but when tucked in, the person is able to increase their speed of spinning. This can be seen in the spinning alligator when the legs are tucked in close to its body. Because the legs play no role in actually producing the torque of the spin, it appears that the alligator relies completely on the axial components of its body. The mechanics of the spinning behavior indicate that orientation between the body and tail and, to a lesser extent, the head are important in the maneuver of the alligator. The angular displacement between body parts changes the moment of inertia, which is necessary to conserve angular momentum during the spin. McIlhenny originally noted the reorientation of the tail and tucking of the legs during the roll (McIlhenny, 1935).

The angular momentum balance and lack of external torques to maintain the maneuver make spinning of the alligator a zero angular momentum maneuver. A similar maneuver is observed in an inverted cat during free-fall (Frohlich, 1980; Galli, 1995). The cat in an inverted position is able to twist its body in mid air to land on its feet. The cat begins its free fall with no initial angular momentum (Arabyan and Tsai, 1998). As it falls, the cat bends at the waist. The anterior and posterior body sections rotate in the same direction (Frohlich, 1980; Fredrickson, 1989). Each section has an angular momentum, whose vector sum gives a counter-rotation to the entire body (Edwards, 1986). This results in no net change in angular momentum for the cat. The legs are positioned close to the symmetry axis of each body section during the maneuver. This orientation reduces the moment of inertia and increases the spin rate of the body sections. When the cat has rotated 180°, it straightens its spine to stop rotating and can land on its feet (Fredrickson, 1989). The cat then terminates its maneuver with no angular momentum. The alligator and the cat both generate internal forces that enable these animals to spin.

Generation of shear force in the death roll

To tear apart its food using the death roll, the alligator needs to generate large shear forces. Although data on the magnitude of shear forces required to dismember bodies have not been collected, the shear force in a death roll can be calculated over a range of sizes for the alligator. To illustrate this computation, the morphometric data (Table 1) of a model juvenile (0.3 m) and adult (3 m) specimen of *A. mississippiensis* are used. The calculation estimates the total rotational kinetic energy (K_{rot}) in the spinning maneuver. K_{rot} equals the work needed to remove that energy and bring the roll to a halt.

K_{rot} of an alligator executing a spin possesses two contributions: (1) the rotation at relatively high angular speed of each body section about their individual symmetry axis, ω, and (2) the rotation of the entire animal about the roll axis, ω_{rev}, which occurs at a relatively smaller angular speed. The ratio of ω to ω_{rev} is given by Eqn 13. For the model adult individual, ω/ω_{rev}=11.5 and for the juvenile, ω/ω_{rev}=12.2.

Using ω=1 rotation s^{-1} (=6.3 rad s^{-1}) for our sample calculation, ω_{rev}=(6.3 rad s^{-1})/11.5=0.55 rad s^{-1} and the total rotational kinetic energy K_{rot} of an adult is:

$$K_{rot} = \tfrac{1}{2}\omega^2(i_H+i_B+i_T) + \tfrac{1}{2}\omega_{rev}^2(I_H+I_B+I_T) = 75.6\ \text{J} + 2.5\ \text{J} = 78.1\ \text{J}\ . \quad (14)$$

Note that the kinetic energy involved in the obvious spinning motion around the symmetry axes of each body part is substantially larger than the motion around the roll axis.

The work done by a constant external torque Γ acting over an angle θ in order to remove an energy K_{rot} is $W=\Gamma\theta$. For θ=1, rotation=2π rad, in our case, Γ=(78.1 J)/2π=12.4 N m. Furthermore, the shear force produced by this torque acting over a lever arm equal to one half the width (w) of the distal portion of the snout equals the torque, i.e. $\Gamma=F_s(0.5w)$, and therefore $F_s=2\Gamma/w$=(2)(12.1 N m)/(0.18 m)=138 N. This analysis does not account for any reduction in the ultimate strength of the prey's tissue due to perforation by the alligator's dentition, which would serve to significantly lower the shear force required for dismemberment.

For comparison, results for the juvenile *A. mississippiensis* executing a death roll with ω=2 rotations s^{-1} show that ω/ω_{rev}=12.2, which yields, along with relevant data from Table 1, $K_{rot}=4.1\times10^{-4}$ J. The corresponding torques and shear force are 6.5×10^{-5} N m and 0.015 N, respectively. Thus, an adult having a mass 1800 times that of a juvenile can produce 200 000 times the energy and torque, and approximately 1000 times the shear force.

Force scaling relationships of alligators

The foregoing analysis permits the development of a scaling relation for large adult individuals with lengths in the vicinity of 3 m. For 51 individuals ranging in length from 0.23 m to 3.75 m and in mass from 0.0318 kg to 296.7 kg (Fig. 7), mass M varies with length L according to the equation:

$$M = CL^p\ , \quad (15)$$

where C=3.6±0.4 and p=3.24±0.03, obtained by least-squares regression. The 95% confidence interval for the value of p is 3.18–3.30. This interval does not overlap the predicted value of p=3.00 for isometric scaling. The increase in mass of alligators is therefore positively allometric with respect to length. An implication of this relationship is that shear forces will be predicted also to increase with positive allometry.

If we assume that the masses and lengths of the head, body and tail are distributed proportionally as in the individual in

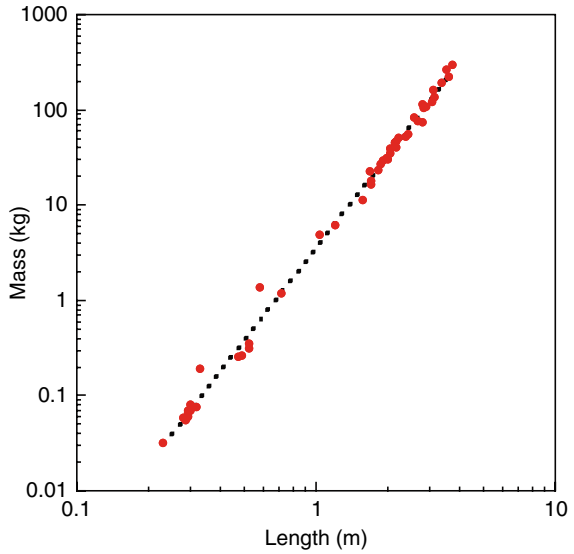

Fig. 7. Scaling relationship between the mass and length of 51 alligators. Data were collected from individuals used in this study and from other sources (McIlhenny, 1935; Joanen and McNease, 1971; Dodson, 1975; Fish, 1984; Erickson et al., 2003). The dotted line shows the regression line (Eqn 15 in text), which was significant (R=0.99; P<0.001).

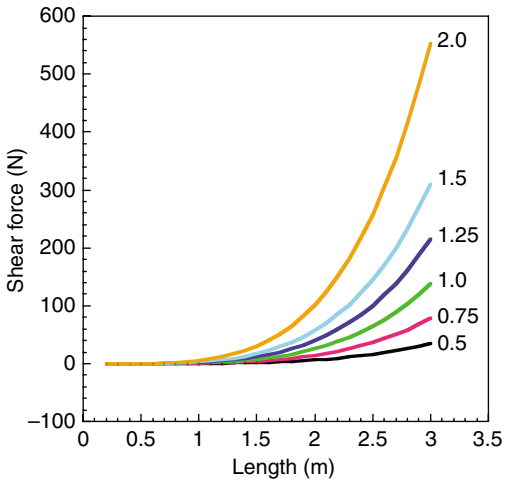

Fig. 8. Calculated shear force as a function of total length of alligators. The lines for shear force were based on Eqn 17 for a combination of rotation rates (rotations s^{-1}) and body lengths.

Table 1, the various moments of inertia can be determined in terms of the total length. These results, in turn, can be used in Eqn 14 to write K_{rot} in terms of the length of the alligator and its angular rate of rotation as:

$$K_{rot} = 6.68\times10^{-3}\omega^2 L^{5.24}\,, \qquad (16)$$

where K_{rot} is in joules (J). The shear force F_s (in N) corresponding to this energy is:

$$F_s = 0.0354\omega^2 L^{4.24}\,, \qquad (17)$$

where growth of the skull and snout is assumed to be isometric (Dodson, 1975). Using Eqn 15, Eqn 17 can be rewritten so that the shear force is given in terms of mass:

$$F_s = 6.62\times10^{-3}\omega^2 M^{1.31}\,. \qquad (18)$$

The shear force is extremely sensitive to changes in size of the alligator (Fig. 8). For example, for the same ω (rad s^{-1}), an adult whose length is just 10% larger than another whose length is 3 m produces a shear force 50% greater. Helfman and Clark (Helfman and Clark, 1986) provide values for ω of 0.6–1.1 rotations s^{-1} for large (>3 m) crocodiles. Using ω=1 rotation s^{-1}=6.3 rad s^{-1}, the record alligator of 5.8 m (Wood, 1976) would have a F_s of 2326 N! Thus, shear forces generated by the spinning maneuver are predicted to increase disproportionally with alligator size, allowing dismemberment of large prey.

Along with crocodilians, spin feeding is used by other vertebrates with elongate bodies (Gans, 1974; Helfman and Clark, 1986; Measey and Herrel, 2006). Among these other species, spinning by eels occurs at higher rotation rates than similarly sized alligators and the mechanics of spinning may be different. A spinning force of 1.35 N was measured on rotationally feeding caecilians (Measey and Herrel, 2006). Although this spinning force was greater than the shear force calculated for alligators of approximately the same body length, these forces are not equivalent. The caecilians were handheld and were presumably pushing off the solid substrate during the maneuver, whereas alligators can generate their own internal torques to spin in water.

Rolling has largely been ignored as a maneuver for animals. Analyses of maneuverability and agility have been confined to examination of pitching and yawing motions (Frey and Salisbury, 2000; Webb, 2002; Fish, 2002; Rivera et al., 2006). While pitch and yaw are typically associated with directional changes during locomotion, roll is used for more varied behaviors. Spinner dolphins (*Stenella longirostris*) perform aerial leaps and rotate around their longitudinal axis up to seven times. This behavior was believed to function in the removal of remoras from the body surface (Fish et al., 2006), but may function in acoustic communication. Birds will roll to use a component of lift generated by the wings to produce a centripetal force to effect turning in flight (Norberg, 1990). Similarly, turning in water is facilitated by rolling in marine mammals and penguins (Hui, 1995; Fish and Battle, 1995; Fish, 2002; Fish et al., 2003; Cheneval et al., 2007). Kasapi et al. (Kasapi et al., 1993) considered roll to be an important kinematic parameter in escape maneuvers by knifefish (*Xenomystus nigri*). Female dugongs (*Dugon dugon*) and right whales (*Eubalaena australis*) will roll onto their backs at the water surface to prevent mating with unwanted suitors (Payne, 1995; Marsh, 2002). Grooming by sea otters (*Enhydra lutris*) utilizes rolling to wash the fur (Kenyon, 1969). Rolling maneuvers are also involved in feeding behaviors. Fin whales (*Balaenoptera physalus*) and other rorquals make lateral lunges involving a 90° roll (Goldbogen et al., 2006). Gray whales (*Eschrichtius robustus*) consume benthic invertebrates (Pivorunas, 1979) by laterally orienting the body as they plow thorough the soft sediment. The varied nature of these behaviors provide a fruitful avenue for future studies of maneuvering performance.

List of symbols and abbreviations

a_B, a_H	semi-major axis of model ellipsoidal body and head; length=2*a*
b_B, b_H	semi-minor axes of model ellipsoidal body and head; width=2*b*
C	proportionality constant in power law relation between *L* and *M*
d	perpendicular distance of snout tip to symmetry axis of body
F_s	shear force at snout
i_B, i_H, i_T	smallest value of the principal moments of inertia for the body, head and tail, respectively
I_B, I_H, I_T	largest value of the principal moments of inertia for the body, head and tail, respectively
K_{rot}	rotational kinetic energy
l_T	length of model right circular cone tail
L	total length of alligator
L_B, L_H, L_T	angular momenta of body, head and tail, respectively
m_B, m_H, m_T	masses of the body, head and tail, respectively
M	total mass of alligator
p	exponent in power law relation between *L* and *M*
r	radius of model right circular cone tail
RR′	roll axis
w	width
$\hat{x}$,$\hat{y}$	unit vectors for each body part in Cartesian coordinates
θ	angle between symmetry axis of head and roll axis
ϕ	angle between symmetry axis of tail and roll axis
Γ	torque
ω	angular rate of rotation around symmetry axis of body part
ω_{rev}	angular rate of rotation of alligator around roll axis

We would like to express our appreciation to the Lauder Laboratory, Harvard University for providing morphometrics data and to the two anonymous viewers for their helpful comments on the manuscript. All experiments with the alligators were in compliance with the West Chester University Institution Animal Care and Use Committee.

References

Arabyan, A. and Tsai, D. (1998). A distributed control model for the air-righting reflex of a cat. *Biol. Cybern*. **79**, 393-401.

Cheneval, O., Blake, R. W., Trites, A. W. and Chan, K. H. S. (2007). Turning maneuvers in Stellar sea lions (*Eumatopias jubatus*). *Mar. Mamm. Sci.* **23**, 94-109.

Cleuren, J. and De Vree, F. (1992). Kinematics of the jaw and hyolingual apparatus during feeding in *Caiman crocodilus*. *J. Morphol*. **221**, 141-154.

Cleuren, J. and De Vree, F. (2000). Feeding in crocodilians. In *Feeding: Form, Function, and Evolution in Tetrapod Vertebrates* (ed. K. Schwenk), pp. 337-358. San Diego: Academic Press.

Currey, J. D. (2002). *Bones: Structure and Mechanics*. Princeton: Princeton University Press.

Davenport, J., Grove, D. J., Cannon, J., Ellis, T. R. and Stables, R. (1990). Food capture, appetite, digestion rate and efficiency in hatchling and juvenile *Crocodylus porosus. J. Zool. Lond*. **220**, 569-592.

Dodson, P. (1975). Functional significance of relative growth in *Alligator*. *J. Zool. Lond.* **175**, 315-355.

Edwards, M. H. (1986). Zero angular momentum turns. *Am. J. Phys*. **54**, 846-847.

Erickson, G. M., Lappin, A. K. and Vliet, K. A. (2003). The ontogeny of bite-force performance in American alligator (*Alligator mississippiensis*). *J. Zool. Lond.* **260**, 317-327.

Fish, F. E. (1984). Kinematics of undulatory swimming in the American alligator. *Copeia* **1984**, 839-843.

Fish, F. E. (2002). Balancing requirements for stability and maneuverability in cetaceans. *Integr. Comp. Biol.* **42**, 85-93.

Fish, F. E. and Battle, J. M. (1995). Hydrodynamic design of the humpback whale flipper. *J. Morphol.* **225**, 51-60.

Fish, F. E., Hurley, J. and Costa, D. P. (2003). Maneuverability by the sea lion, *Zalophus californianus*: turning performance of an unstable body design. *J. Exp. Biol.* **206**, 667-674.

Fish, F. E., Nicastro, A. J. and Weihs, D. (2006). Dynamics of the aerial maneuvers of spinner dolphins. *J. Exp. Biol.* **209**, 590-598.

Fredrickson, J. E. (1989). The tail-less cat in free-fall. *Physiol. Teach*. **27**, 620-624.

Frey, E. and Salisbury, S. W. (2000). The kinematics of aquatic locomotion in *Osteolaemus tetraspis* Cope. In *Crocodilian Biology and Evolution* (ed. G. C. Griggs, F. Seebacher and C. E. Franklin), pp. 165-179. Chipping Norton: Surry Beatty & Sons.

Frohlich, C. (1979). Do springboard divers violate angular momentum conservation? *Am. J. Phys*. **47**, 583-592.

Frohlich, C. (1980). The physics of somersaulting and twisting. *Sci. Am*. **242**, 154-164.

Galli, J. R. (1995). Angular momentum conservation and the cat twist. *Physiol. Teach*. **33**, 404-407.

Gans, C. (1974). *Biomechanics: An Approach to Vertebrate Biology*. Philadelphia: J. B. Lippincott.

Giancoli, D. C. (1985). *Physics*. Englewood Cliffs, NJ: Prentice Hall.

Goldbogen, J. A., Camalbokidis, J., Shadwick, R. E., Oleson, E. M., McDonald, M. A. and Hildebrand, J. A. (2006). Kinematics of foraging dives and lunge-feeding in fin whales. *J. Exp. Biol.* **209**, 1231-1244.

Gordon, J. E. (1978). *Structures: or Why Things Don't Fall Down*. New York: Da Capo.

Gray, D. E. (1963). *American Institute of Physics Handbook* (2nd edn). New York: McGraw-Hill.

Guggisberg, C. A. W. (1972). *Crocodiles: Their Natural History, Folklore and Conservation*. Harrisburg: Stackpole Books.

Helfman, G. S. and Clark, J. B. (1986). Rotational feeding: overcoming gape-limited foraging in anguillid eels. *Copeia* **1986**, 679-685.

Hui, C. A. (1985). Maneuverability of the Humboldt penguin (*Spheniscus humboldti*) during swimming. *Can. J. Zool*. **63**, 2165-2167.

Joanen, T. and McNease, L. (1971). Propagation of the American alligator in captivity. *Proc. Annu. Conf. S. E. Assoc. Game Fish Comm*. **25**, 106-116.

Kane, T. R. and Scher, M. P. (1970). Human self-rotation by means of limb movements. *J. Biomech*. **3**, 39-49.

Kasapi, M. A., Domenici, P. D., Blake, R. W. and Harper, D. G. (1993). The kinematics and performance of the escape response of the knifefish, *Xenomystus nigri*. *Can. J. Zool*. **71**, 189-195.

Kenyon, K. W. (1969). The sea otter in the eastern Pacific Ocean. *N. Am. Fauna* **68**, 1-352.

Marsh, H. (2002). Dugong. In *Encyclopedia of Marine Mammals* (ed. W. F. Perrin, B. Würsig and J. G. M. Thewissen), pp. 344-347. San Diego: Academic Press.

McIlhenny, E. A. (1935). *The Alligator's Life History*. Boston: Christopher Publishing House.

Measey, G. J. and Herrel, A. (2006). Rotational feeding in caecilians: putting a spin on the evolution of cranial design. *Biol. Lett*. **2**, 485-487.

Neill, W. T. (1971). *The Last of the Ruling Reptiles: Alligators, Crocodiles, and Their Kin*. New York: Columbia University Press.

Norberg, U. M. (1990). *Vertebrate Flight: Mechanics, Physiology, Morphology, Ecology and Evolution*. Berlin: Springer-Verlag.

Payne, R. (1995). *Among Whales*. New York: Scribner.

Pivorunas, A. (1979). The feeding mechanisms of baleen whales. *Am. Sci*. **67**, 432-440.

Pooley, A. C. and Gans, C. (1976). The Nile crocodile. *Sci. Am*. **234**, 114-124.

Rivera, G., Rivera, A. R. V., Dougherty, E. E. and Blob, R. W. (2006). Aquatic turning performance of painted turtles (*Chrysemys picta*) and functional consequences of a rigid body design. *J. Exp. Biol.* **209**, 4203-4213.

Ross, C. A. (1989). *Crocodiles and Alligators*. New York: Facts On File.

Webb, P. W. (2002). Control of posture, depth, and swimming trajectories of fishes. *Integr. Comp. Biol*. **42**, 94-101.

Wood, G. L. (1976). *The Guinness Book of Animal Facts and Feats*. Enfield: Guinness Superlatives.